

Fluorescence Spectra of Eu(II) in Borate and Aluminate Glasses

Katsuhisa TANAKA,* Tomohito OHYAGI, Kazuyuki HIRAO, and Naohiro SOGA

Department of Industrial Chemistry, Faculty of Engineering, Kyoto University, Sakyo-ku, Kyoto 606-01

(Received November 2, 1992)

The fluorescence and ^{151}Eu Mössbauer spectra have been obtained for alkali borate, alkaline earth borate and rare-earth aluminate glasses containing Eu^{2+} ions. The Mössbauer spectra indicate that about 70 to 80% of the europium ions are present as Eu^{2+} ions in the borate glasses. As for the aluminate glasses, almost all of the europium ions are present as Eu^{2+} ions. The fluorescence spectra due to the $4f^65d^1 \rightarrow 4f^7$ transition of the Eu^{2+} ion have been observed under excitation with UV radiation. There exists an empirical relationship that the emission energy decreases monotonically with an increase in the theoretical optical basicity of glass, irrespective of the glass systems. This relationship is explained in terms of simple crystal field theory by assuming that the splitting of the 5d levels mainly determines the emission energy of the Eu^{2+} ions. This empirical relationship also indicates that Eu^{2+} ions are distributed rather homogeneously in the present borate and aluminate glasses.

Oxide and fluoride glasses containing Eu^{2+} ions are interesting materials from the viewpoint of their magnetic and optical properties. A glass containing a large amount of Eu^{2+} ions shows a Faraday effect with a large Verdet constant in the visible light region. Shafer and Suits¹⁾ obtained $-2.55 \text{ min Oe}^{-1} \text{ cm}^{-1}$ ($1 \text{ Oe} = 1000/4\pi \text{ A m}^{-1}$) as the Verdet constant at an incident light of 450 nm for $34.2\text{EuO} \cdot 14.8\text{Al}_2\text{O}_3 \cdot 50.7\text{B}_2\text{O}_3$ glass. This value is larger than those for borate²⁾ and phosphate³⁾ glasses containing trivalent rare-earth ions. Schoenes et al.⁴⁾ carried out magnetic and magneto-optical measurements on $\text{Eu}_{0.14}\text{Si}_{0.31}\text{O}_{0.55}$ glass in order to clarify whether spin glass or a micromagnetic transition can take place or not in the case that a long-range magnetic interaction, such as Ruderman–Kittel–Kasuya–Yosida (RKKY) interaction, is absent. The concentration of Eu^{2+} ions was estimated to be 12 at % (atomic percent) in this glass; most of the europium ions are present as Eu^{2+} ions. Low-field magnetization measurements indicated that a freezing of spins does not occur above 1.5 K. Also, they observed optical absorption at around 500 nm due to the $4f^7 \rightarrow 4f^65d^1$ transition of the Eu^{2+} ion, and a Faraday rotation based on this transition in this glass.

The chemical structure around Eu^{2+} ions incorporated in glasses has already been investigated by means of optical absorption measurements and ^{151}Eu Mössbauer spectroscopy. Shafer and Perry⁵⁾ examined the optical absorption spectra of Eu^{2+} in $\text{ZrF}_4\text{–BaF}_2\text{–ThF}_4$ glasses. By comparing the absorption spectra of the fluoride glasses with those of several oxide and fluoride crystals such as EuO , EuF_2 , $\text{RbCaF}_3\text{:Eu}^{2+}$, and $\text{BaLiF}_3\text{:Eu}^{2+}$, they concluded that the average coordination number for the Eu^{2+} ion is 12. ^{151}Eu Mössbauer measurements were carried out by Coey et al.⁶⁾ indicating that about 90% of the europium ions are present as Eu^{2+} in these fluorozirconate glasses. They also evaluated the coordination number for the Eu^{2+} ion to be 8 to 12 based on the isomer shift. Winterer et al.⁷⁾ prepared alkali borate glasses containing several concentrations of Eu^{2+} ions and performed Mössbauer mea-

surements at 300 and 4.2 K. They found that Eu^{2+} ions are distributed rather homogeneously as a network-modifying cation in the glass and that the spin-lattice relaxation is almost independent of the temperature, because 4f electrons are shielded rather strongly by the outer orbitals.

Glass containing a small amount of Eu^{2+} ions is a promising material as a fluorescent substance; Eu^{2+} ion can emit radiation in the blue-to-green region, which corresponds to the $4f^65d^1 \rightarrow 4f^7$ transition.⁸⁾ To our knowledge, however, few systematic investigations have been reported concerning the fluorescence spectra of the Eu^{2+} ion in oxide glasses, particularly, concerning the relationship between the fluorescence spectra and the chemical structures around the Eu^{2+} ions. In the present investigation, Eu^{2+} -containing alkali borate, alkaline earth borate and rare-earth aluminate glasses were prepared by using a twin-roller method as well as a conventional melting-and-quenching method; the fluorescence spectra of these glasses were examined. ^{151}Eu Mössbauer measurements were also carried out in order to mainly obtain information concerning the fraction of Eu ions in the divalent state in these glasses. We show that the emission energy due to the $4f^65d^1 \rightarrow 4f^7$ transition is describable in terms of the theoretical optical basicity of glass with the aid of simple crystal field theory for the present borate and aluminate glasses.

Experimental

Sample Preparation. Eu^{2+} -containing glasses were prepared by melting mixtures of oxides, including Eu_2O_3 , under reducing conditions, following the method by Winterer et al.⁷⁾ Reagent-grade Li_2CO_3 , Na_2CO_3 , K_2CO_3 , CaCO_3 , SrCO_3 , BaCO_3 , B_2O_3 , Y_2O_3 , La_2O_3 , Gd_2O_3 , Al_2O_3 , and Eu_2O_3 were used as starting materials. For the borate systems, the raw materials were weighed in the prescribed compositions given in Table 1, so that the total weight was 15 g. Then, 0.05 to 0.15 g of carbon powders was added to the mixture of oxides as a reducing agent; they were then mixed thoroughly. The mixture was put into an alumina crucible and melted in a electric furnace at 1300°C for 1 h in a N_2 atmosphere. For the alkali borate

Table 1. Glass Compositions Represented According to the Molar Ratio

Alkali borate	
$x\text{Li}_2\text{O} \cdot (100-x)\text{B}_2\text{O}_3 \cdot 1\text{EuO}$	$x=10, 15, 20, 25, 30$
$x\text{Na}_2\text{O} \cdot (100-x)\text{B}_2\text{O}_3 \cdot 1\text{EuO}$	$x=10, 15, 20, 25, 30$
$x\text{K}_2\text{O} \cdot (100-x)\text{B}_2\text{O}_3 \cdot 1\text{EuO}$	$x=10, 15, 20, 25, 30$
$30\text{Li}_2\text{O} \cdot 70\text{B}_2\text{O}_3 \cdot x\text{EuO}$	$x=0.1, 0.5, 1, 3, 5$
Alkaline earth borate	
$30\text{CaO} \cdot 70\text{B}_2\text{O}_3 \cdot 1\text{EuO}$	
$30\text{SrO} \cdot 70\text{B}_2\text{O}_3 \cdot 1\text{EuO}$	
$30\text{BaO} \cdot 70\text{B}_2\text{O}_3 \cdot 1\text{EuO}$	
Rare-earth aluminate	
$20\text{Y}_2\text{O}_3 \cdot 80\text{Al}_2\text{O}_3 \cdot 1\text{EuO}$	
$20\text{La}_2\text{O}_3 \cdot 80\text{Al}_2\text{O}_3 \cdot 1\text{EuO}$	
$20\text{Gd}_2\text{O}_3 \cdot 80\text{Al}_2\text{O}_3 \cdot 1\text{EuO}$	
$33\text{EuO} \cdot 67\text{Al}_2\text{O}_3$	

glasses, the melt was cooled to 400°C, kept for 20 min at 400°C and then cooled to room temperature. For the alkaline earth borate glass, the melt was quenched by pouring it onto a twin-roller made of stainless steel and rotating at about 1000 rpm.

As for the aluminate systems, the starting materials were weighed so that the total weight was 5 g; 0.15 g of carbon powders was added. The mixture was pressed into a bar under hydrostatic pressure and melted in a N₂ atmosphere by using an image furnace with a Xe lamp as the heat source. The melt was quenched by falling onto the twin-roller. Thus, bulk glass was obtained for the alkali borate systems, and glass with a thin foil form of about 20 μm thickness was obtained for the alkaline earth borate and the rare-earth aluminate systems. The resultant specimens were ascertained to be amorphous by using X-ray diffraction analyses with CuKα radiation.

Measurements. The obtained glasses were subjected to fluorescence and ¹⁵¹Eu Mössbauer measurements. These measurements were performed at room temperature. The fluorescence spectra were obtained by using a Hitachi 850 fluorescence spectrometer with a Xe lamp. The excitation wavelength was fixed at 394 nm. The excitation spectra were obtained by monitoring the peak position of the emission. In the ¹⁵¹Eu Mössbauer measurements, 1.85 GBq ¹⁵¹Sm₂O₃ was used as the γ-ray source. The spectrum of EuF₃ was measured as a Doppler velocity standard. Calibration of the velocity was achieved by using the spectrum of α-Fe foil at room temperature.

Results

Fluorescence Spectra. The fluorescence spectra of $x\text{Li}_2\text{O} \cdot (100-x)\text{B}_2\text{O}_3 \cdot 1\text{EuO}$ glasses are shown in Fig. 1. As mentioned below, the fraction of Eu²⁺ ions among the total europium ions was estimated to be about 70 to 80% from the results of the Mössbauer measurements. The emission appears at around 450 nm as a broad spectrum. The emission energy decreases with an increase in the concentration of Li₂O. For the 30Li₂O·70B₂O₃·1EuO glass, a slight peak is observed at around 610 nm. This arises from the ⁵D₀–⁷F₂ transition

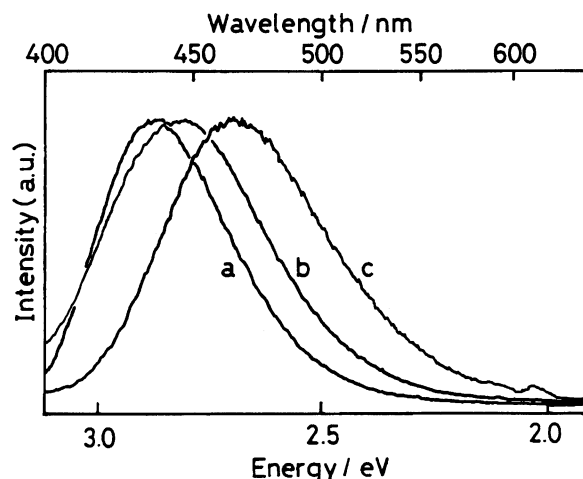


Fig. 1. Fluorescence spectra of $x\text{Li}_2\text{O} \cdot (100-x)\text{B}_2\text{O}_3 \cdot 1\text{EuO}$ glasses with (a) $x=10$, (b) $x=20$, and (c) $x=30$.

of the Eu³⁺ ion which is present in low concentration in the glass. Figure 2 shows the fluorescence spectra of alkali borate glasses with the 30M₂O·70B₂O₃·1EuO composition, where M=Li, Na and K. The peak position of the emission lies in the smallest energy for potassium borate glass and in the largest energy for lithium borate glass. Emission with weak intensity due to the Eu³⁺ ions was also observed for potassium borate glass. Figure 3 shows the fluorescence spectra of the alkaline earth borate glasses. The emission energy decreases in the order Ca>Sr>Ba. The emission due to Eu³⁺ ions was also observed for these glasses. Figure 4 shows the fluorescence spectra of rare-earth aluminate glasses. These glasses could not be prepared unless rapid quenching was applied. In this figure, the fluorescence spectrum of 20Li₂O·80B₂O₃·1EuO glass is also shown for a comparison. It was found that the peak position of the spectra lies in much longer wave-

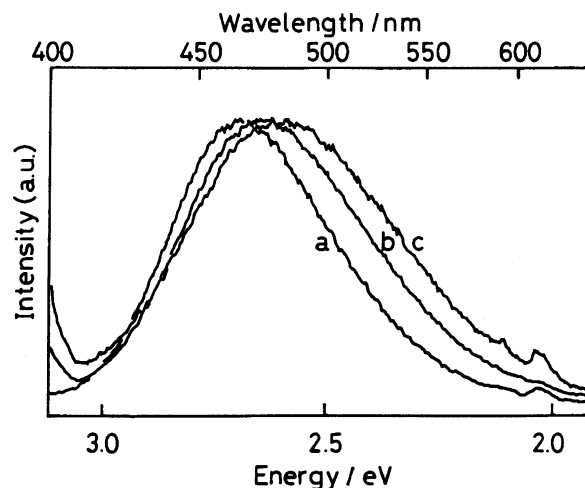


Fig. 2. Fluorescence spectra of (a) 30Li₂O·70B₂O₃·1EuO, (b) 30Na₂O·70B₂O₃·1EuO and (c) 30K₂O·70B₂O₃·1EuO glasses.

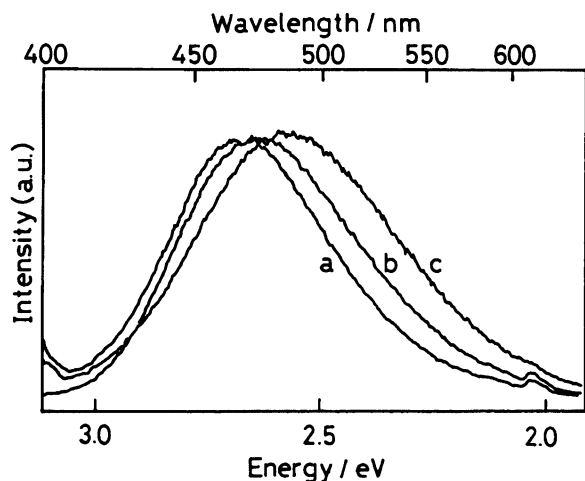


Fig. 3. Fluorescence spectra of (a) $30\text{CaO}\cdot 70\text{B}_2\text{O}_3\cdot 1\text{EuO}$, (b) $30\text{SrO}\cdot 70\text{B}_2\text{O}_3\cdot 1\text{EuO}$, and (c) $30\text{BaO}\cdot 70\text{B}_2\text{O}_3\cdot 1\text{EuO}$ glasses.

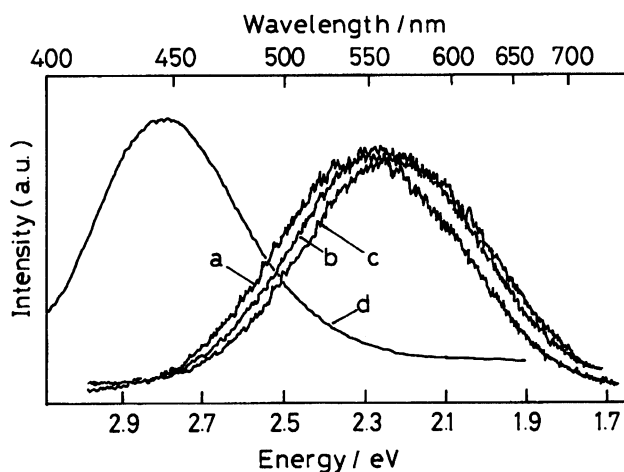


Fig. 4. Fluorescence spectra of (a) $20\text{Y}_2\text{O}_3\cdot 80\text{Al}_2\text{O}_3\cdot 1\text{EuO}$, (b) $20\text{Gd}_2\text{O}_3\cdot 80\text{Al}_2\text{O}_3\cdot 1\text{EuO}$, and (c) $20\text{La}_2\text{O}_3\cdot 80\text{Al}_2\text{O}_3\cdot 1\text{EuO}$ glasses. The fluorescence spectrum of (d) $20\text{Li}_2\text{O}\cdot 80\text{B}_2\text{O}_3\cdot 1\text{EuO}$ glass is also shown for a comparison.

length region for rare-earth aluminate glasses than for the $20\text{Li}_2\text{O}\cdot 80\text{B}_2\text{O}_3\cdot 1\text{EuO}$ glass. The above emission spectra are assigned to the transition from $4f^65d^1$ to $4f^7$.⁸⁾

The excitation spectra of $10\text{Li}_2\text{O}\cdot 90\text{B}_2\text{O}_3\cdot 1\text{EuO}$ and $30\text{Li}_2\text{O}\cdot 70\text{B}_2\text{O}_3\cdot 1\text{EuO}$ glasses are shown in Fig. 5. The emission at 420 and 460 nm was monitored for these glasses, respectively. For the latter glass, four peaks were observed in the broad spectrum. These peaks are indicated by arrows in this figure. These four peaks correspond to the transitions of electrons from the 4f orbital to the upper four levels of the 5d orbitals. The broadness of the spectra indicates that the site-to-site distribution of Eu^{2+} ions is large in the glass. In particular, for the $10\text{Li}_2\text{O}\cdot 90\text{B}_2\text{O}_3\cdot 1\text{EuO}$ glass, the spectrum is so broad that the four peaks are barely distinguish-

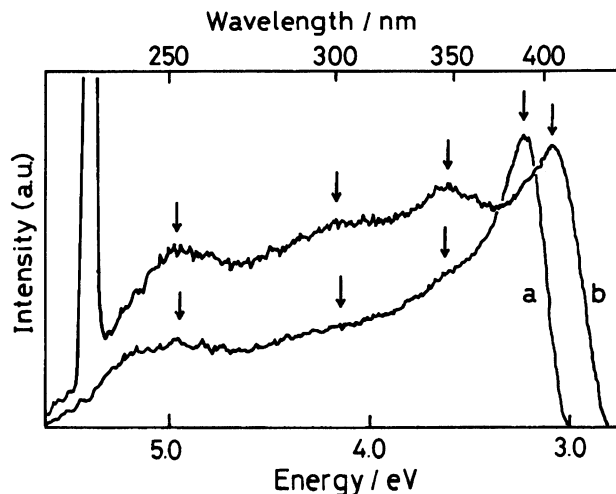


Fig. 5. Excitation spectra of (a) $10\text{Li}_2\text{O}\cdot 90\text{B}_2\text{O}_3\cdot 1\text{EuO}$ and (b) $30\text{Li}_2\text{O}\cdot 70\text{B}_2\text{O}_3\cdot 1\text{EuO}$ glasses. The emission at 420 and 460 nm was monitored for these glasses, respectively. Intense absorption takes place at 230 nm in the spectrum of the $30\text{Li}_2\text{O}\cdot 70\text{B}_2\text{O}_3\cdot 1\text{EuO}$ glass, since radiation at 230 nm interferes with each other to yield radiation with one half the energy, that is, 460 nm.

able from one another.

Mössbauer Spectra. Figure 6 shows the Mössbauer spectra of $30\text{Li}_2\text{O}\cdot 70\text{B}_2\text{O}_3\cdot x\text{EuO}$ glasses with $x = 1, 3$, and 5. In addition to the absorption peak due to Eu^{2+} ions, absorption due to Eu^{3+} ions clearly appears in all of the spectra. The fraction of the absorption area of Eu^{2+} ions in the total absorption area was estimated to be about 70% for $30\text{Li}_2\text{O}\cdot 70\text{B}_2\text{O}_3\cdot 1\text{EuO}$, and about 80% for $30\text{Li}_2\text{O}\cdot 70\text{B}_2\text{O}_3\cdot 3\text{EuO}$ and $30\text{Li}_2\text{O}\cdot 70\text{B}_2\text{O}_3\cdot 5\text{EuO}$ glasses. As pointed out by Coey et al.,⁶⁾ the absorption area ratio is not exactly equal to the ratio of the number of Eu^{2+} ions to that of the Eu^{3+} ions, because the absorption area is influenced by the recoil-free fraction. In order to estimate the amount of both ions more accurately, it is necessary to analyze the temperature dependence of the absorption area under an appropriate model for the vibrational density of state, as performed by Tanaka et al. for amorphous iron alloys.^{9,10)} Coey et al.⁶⁾ analyzed the temperature dependence of the absorption area by assuming the Debye model, revealing that the Debye temperature for Eu^{2+} ions is smaller than that for Eu^{3+} ions. If this is also the case for the present lithium borate glasses, the amount of Eu^{2+} ions is larger than that expected from the absorption area ratio. It may be concluded that more than 70 to 80% of the europium ions are present as Eu^{2+} ions in the present $30\text{Li}_2\text{O}\cdot 70\text{B}_2\text{O}_3$ glasses.

The linewidth of the absorption peak for Eu^{2+} ions is much broader than that for Eu^{3+} ions in all of the glasses. This is due to the hyperfine structure of the Eu^{2+} ions.⁷⁾ The splitting of the peaks due to hy-

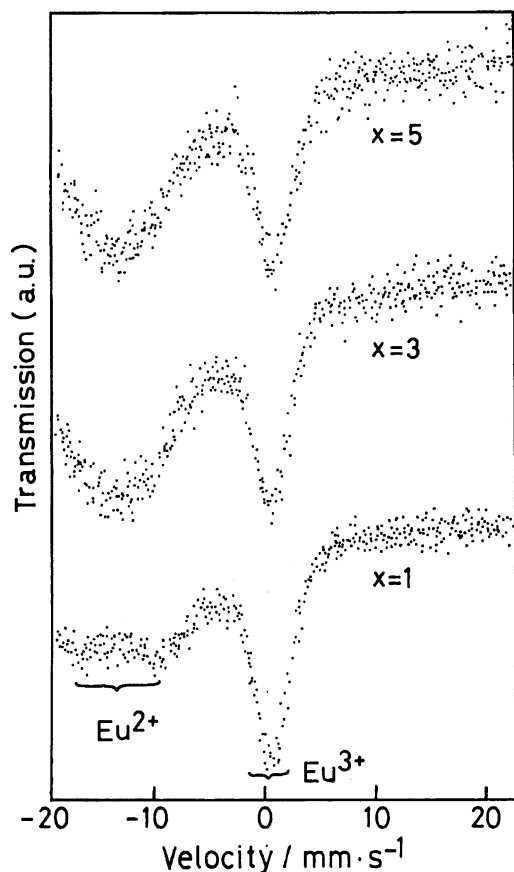


Fig. 6. Mössbauer spectra of $30\text{Li}_2\text{O}\cdot 70\text{B}_2\text{O}_3\cdot x\text{EuO}$ glasses with $x=1, 3$, and 5 .

perfine fields is clearly observed in the spectrum of $30\text{Li}_2\text{O}\cdot 70\text{B}_2\text{O}_3\cdot 1\text{EuO}$ glass. This indicates that the Eu^{2+} ions are distributed rather homogeneously in this glass. As the concentration of Eu^{2+} ions is increased, the hyperfine structure becomes ambiguous. The increase in the concentration makes the spacing between Eu^{2+} ions shorter. As a result, the hyperfine structure becomes ambiguous because of a spin-spin relaxation process from dipolar interactions among Eu^{2+} ions.

Figure 7 shows the Mössbauer spectrum of $33\text{EuO}\cdot 67\text{Al}_2\text{O}_3$ glass. It can be seen that all of the europium ions are present as Eu^{2+} ions in this glass. The hyperfine structure can barely be observed because of the high concentration of Eu^{2+} ions.

Discussion

The variation of the peak position of the fluorescence spectrum with glass composition shown in Figs. 1, 2, 3, and 4 implies that the emission energy is related to the basicity of the glass. Thus, for the present glasses, we calculated the theoretical optical basicity proposed by Duffy and Ingram,¹¹⁾ and examined the relationship between the emission energy and the optical basicity of the glasses. According to Duffy and Ingram, the theoretical optical basicity is defined as follows,¹¹⁾

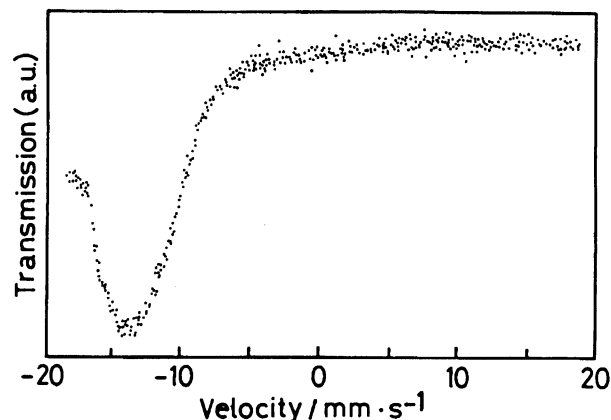


Fig. 7. Mössbauer spectrum of $33\text{EuO}\cdot 67\text{Al}_2\text{O}_3$ glass.

$$A = 1 - \sum_i (z_i r_i / 2) (1 - 1/\gamma_i), \quad (1)$$

where z_i is the valence of the i -th cation, r_i is the ratio of the number of i -th cations to that of oxide ions, and γ_i is a basicity moderating parameter, defined as

$$\gamma_i = 1.36 (\chi_i - 0.26), \quad (2)$$

where χ_i is the electronegativity of Pauling for the i -th atom. Duffy and Ingram¹¹⁾ showed that there exists a good correlation between the theoretical optical basicity and the experimental optical basicity, which was determined from the absorption due to the $^1\text{S}_0 \rightarrow ^3\text{P}_1$ transition for Pb^{2+} ions incorporated in several oxide glasses, sulfate glasses, H_2SO_4 , H_3PO_4 , and CaO . We calculated the theoretical optical basicity of the borate and aluminate glasses by using Eqs. 1 and 2; the emission energy is plotted against the optical basicity in Fig. 8. In the calculation, the electronegativity of Allred and Rochow^{12,13)} as well as the electronegativity of Pauling was used, since the former gives more available data. Presumably, the use of the electronegativity of Allred and Rochow does not cause any serious discrepancy, since it was derived using the electronegativity of Pauling. Figure 8 shows that the emission energy decreases monotonically as the theoretical optical basicity of glass increases, irrespective of the glass systems.

The emission energy due to the transition from $4f^6 5d^1$ to $4f^7$ is influenced by both the electron-phonon coupling strength and the splitting of the 5d levels. The larger Stokes' shift results in a smaller emission energy. Also, the larger splitting of the 5d levels results in a smaller emission energy, as schematically illustrated in Fig. 9. The splitting of the 5d levels is influenced by the basicity of the glass, because the basicity represents the power of donation of electrons which interact with 5d electrons. When we assume simple crystal field theory, the relationship between the emission energy and the optical basicity of the glass can be qualitatively ex-

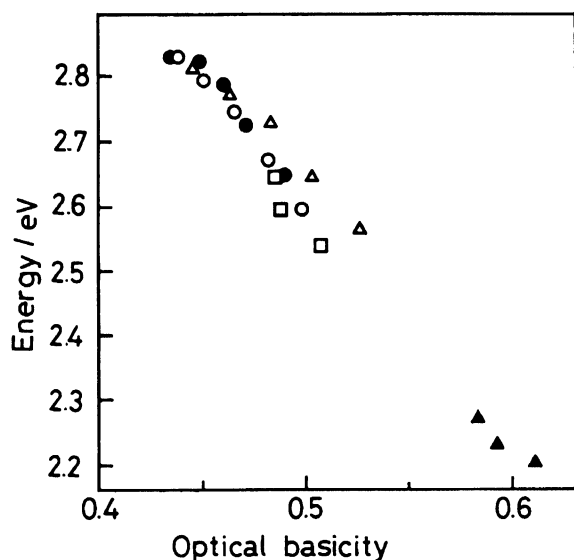


Fig. 8. Relationship between the emission energy and theoretical optical basicity for the present alkali borate, alkaline earth borate, and rare-earth aluminate glasses. ●: $x\text{Li}_2\text{O} \cdot (100-x)\text{B}_2\text{O}_3 \cdot 1\text{EuO}$, ○: $x\text{Na}_2\text{O} \cdot (100-x)\text{B}_2\text{O}_3 \cdot 1\text{EuO}$, △: $x\text{K}_2\text{O} \cdot (100-x)\text{B}_2\text{O}_3 \cdot 1\text{EuO}$, □: $30\text{MO} \cdot 70\text{B}_2\text{O}_3 \cdot 1\text{EuO}$ ($\text{M} = \text{Ca}, \text{Sr}, \text{Ba}$), ▲: $20\text{Ln}_2\text{O}_3 \cdot 80\text{Al}_2\text{O}_3 \cdot 1\text{EuO}$ ($\text{Ln} = \text{Y}, \text{La}, \text{Gd}$).

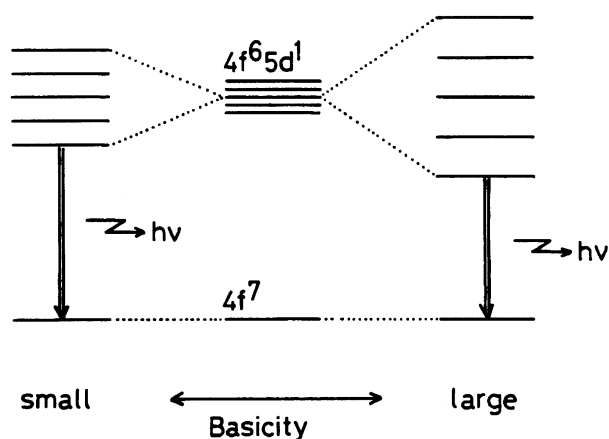


Fig. 9. Schematic illustration of the energy diagram of the 5d orbitals for the Eu^{2+} ion. Individual 5d orbitals are separated from each other because of the asymmetrical coordination state of the oxide ions. The splitting of the 5d levels increases with an increase in the basicity of the glass.

plained by taking into account only the effect of the splitting of the 5d levels. An increase in the optical basicity brings about an increase in the electron density at the oxide ions which coordinate the Eu^{2+} ion. As a result, the splitting of the 5d levels becomes large according to the simple crystal field theory, leading to a decrease in the emission energy, because the emission initiates the lowest 5d level. This situation is presented in Fig. 9. The fact that emission takes place accompanied by a transition from the lowest 5d level to the

$4f^7$ state is demonstrated from the excitation spectra shown in Fig. 5. It is also believed that individual 5d orbitals are separated from each other because of the asymmetrical coordination state of the oxide ions. This is also demonstrated from the excitation spectra shown in Fig. 5. Hence, Fig. 8 seems to show that the emission energy in the green-to-blue region from the Eu^{2+} ions is mainly governed by the average optical basicity of glass in the present borate and aluminate glasses.

The theoretical optical basicity introduced by Eqs. 1 and 2 is a parameter which reflects only the average structure of the glasses. Therefore, if the Eu^{2+} ions are apt to take preferential sites rather than are distributed homogeneously in the glass, the splitting of the 5d levels is more influenced by the local environment around the Eu^{2+} ion than by the average glass structure, leading to no correlation between the emission energy and the optical basicity. In other words, Fig. 8 indicates that the Eu^{2+} ions are distributed rather homogeneously in the present borate and aluminate glasses. For alkali borate glasses, this speculation is coincident with the conclusion derived from Mössbauer measurements carried out by Winterer et al.,⁷⁾ as mentioned above. Also, in Fig. 8, the data for alkali borate, alkali earth borate and rare-earth aluminate glasses align on almost the same line. In other words, the local structure around the Eu^{2+} ions reflects the average glass structure in the present alkali borate, alkali earth borate, and rare-earth aluminate glasses, even though the glass systems are different. There still remains a question as to how the emission energy changes with the theoretical optical basicity in other glass systems, such as silicate and phosphate.

The fraction of Eu^{2+} ions in the total europium ions is 70 to 80% in the alkali borate glasses; it is almost 100% in the aluminate glasses, as revealed from the Mössbauer spectra. The difference in the fraction of Eu^{2+} ions mainly arises from the difference in the melting temperature. Since the melting temperatures of aluminate glasses are higher than those of alkali borate glasses, the fraction of Eu^{2+} ions, i.e., the reduction state, is larger in the aluminate glasses.

References

- 1) M. W. Shafer and J. C. Suits, *J. Am. Ceram. Soc.*, **49**, 261 (1966).
- 2) C. B. Rubinstein, S. B. Berger, L. G. Van Uitert, and W. A. Bonner, *J. Appl. Phys.*, **35**, 2338 (1964).
- 3) S. B. Berger, C. B. Rubinstein, C. R. Kurkjian, and A. W. Treptow, *Phys. Rev.*, **133**, A723 (1964).
- 4) J. Schoenes, E. Kaldis, W. Thöni, and P. Wachter, *Phys. Status Solidi A*, **51**, 173 (1979).
- 5) M. W. Shafer and P. Perry, *Mater. Res. Bull.*, **14**, 899 (1979).
- 6) J. M. D. Coey, A. McEvoy, and M. W. Shafer, *J. Non-Cryst. Solids*, **43**, 387 (1981).
- 7) M. Winterer, E. Mörsen, B. D. Mosel, and W. Müller-Warmuth, *J. Phys. C*, **20**, 5389 (1987).

- 8) G. E. Rindone, "Luminescence of Inorganic Solids," ed by P. Goldberg, Academic Press, New York (1966), p. 432.
 - 9) K. Tanaka, N. Soga, K. Hirao, and K. Kimura, *J. Appl. Phys.*, **60**, 728 (1986).
 - 10) K. Tanaka, K. Hirao, and N. Soga, *J. Appl. Phys.*, **64**, 3299 (1988).
 - 11) J. A. Duffy and M. D. Ingram, *J. Inorg. Nucl. Chem.*, **37**, 1203 (1975).
 - 12) A. L. Allred and E. G. Rochow, *J. Inorg. Nucl. Chem.*, **5**, 264 (1958).
 - 13) E. J. Little and M. M. Jones, *J. Chem. Educ.*, **37**, 231 (1960).
-